A Statewide Deflection Study of Continuously Reinforced Concrete Pavement in Texas

B. F. McCULLOUGH and HARVEY J. TREYBIG
Highway Design Division, Texas Highway Department

This report summarizes a performance study of continuously reinforced concrete pavement in terms of load-deflection studies. In this study the following factors affecting pavement performance were considered: subgrade support, subbase type, concrete modulus of elasticity, concrete modulus of rupture, pavement thickness, season of the year, and soil moisture condition. The effect of each of the factors on the deflection and stress or curvature is discussed.

The variables that significantly affect deflection and radius of curvature are correlated into model equations. The constants in the equations were determined from the data using multiple regression techniques. This study validates some initial assumptions made in the design and development of continuously reinforced concrete pavement for Texas conditions.

•THIS report is a part of a continuing study by the Texas Highway Department pertaining to the development and design of continuously reinforced concrete pavement (CRCP) in Texas. The Texas Highway Department pioneered the use of CRCP in the Southwest with the construction of an experimental pavement in Fort Worth during 1951. Recent reports issued by the Concrete Reinforcing Steel Institute indicate that Texas now has more mileage of CRCP than any other state (1).

During the initial design development stages of CRCP in Texas, several assumptions were made, which the authors wish to reiterate at this point. Among the initial assumptions were the following:

1. To prevent pavement deterioration, the transverse cracks in the pavement must be of small enough magnitude to permit the retention of granular interlock and prevent the entrance of water. If sufficient granular interlock is maintained, then 100 percent load transfer will be experienced across the crack and thus the pavement continuity will be maintained (2).
2. The Westergaard interior loading condition was used for determining the pavement thickness, with additional steel being used at the edge to compensate for the difference in required thickness between an edge and interior loading condition. This approach results in a 1- to 2-in. thinner pavement than would be obtained with normal procedures used in designing jointed concrete pavements (3, 4).

Although the AASHO Road Test provided valuable information for use in the design and construction of rigid pavements, numerous areas remain to be investigated, especially in the field of CRCP, since this pavement type was not covered at the Road Test (5). The deflection data obtained at the AASHO Road Test are difficult to extrapolate to a formula for the design of continuous pavement in Texas because (a) they are not directly applicable to this pavement type, (b) only one natural soil type and strength was considered, (c) only one concrete modulus of elasticity was used, and (d) lime stabilization was not included.

To establish the effect of these parameters and verify the original design assumptions, the Texas Highway Department in 1963 initiated a large research project to

Paper sponsored by Committee on Rigid Pavement Design and presented at the 47th Annual Meeting.

investigate the performance of continuously reinforced concrete pavement. This is the fifth report in connection with this study and the third relating to pavement deflection. The earlier reports pertain to equipment and technique development (6), deflection study on an experimental pavement section (7), and a 24-hour deflection study on several new untrafficked pavements (8).

TABLE 1

SCHEDULE OF FIELD OBSERVATIONS

Run No.	Season	Date Ran
1	Fall	Oct.-Dec. 1963
2	Winter	Jan.-Mar. 1964
3	Summer	June-July 1964
4	Spring	Mar.-Apr. 1965

Since 1963, in excess of 15,000 individual measurements of deflection, radius of curvature, crack width, and temperature have been taken on numerous continuous pavements located throughout the state. The schedule of field observations is given in Table 1. Many of the procedures and techniques used are those developed at the AASHO Road Test or modifications thereof (5, 6). Much work has been done by the Texas Highway Department in developing experimental techniques for studying CRCP.

The overall objective of this investigation is to determine the effects of design variables on pavement deflection and radius of curvature. After establishing the parameters considered to be variables, a statistical expression will be derived that can be used for calculating the deflection and radius of curvature produced by a wheel load on continuous pavement. In addition, the assumptions used in the original design analysis of CRCP will be investigated to determine their validity.

DESCRIPTION OF EXPERIMENT

Factorial Design

The entire experiment was functional through a factorial design that encompassed the variables involved in pavement design. The chart representing the factorial

Subgrade Support	Subbase Type	Subbase Material	Modulus of Elasticity / Concrete Flexural Strength	X = 8" CRCP: 3,500,000 psi — Low 580 psi(−)	X = 8" CRCP: 3,500,000 psi — Medium 580-690 psi	X = 8" CRCP: 3,500,000 psi — High 690 psi(+)	Y = 6" CRCP: 5,500,000 psi — Low 580 psi(−)	Y = 6" CRCP: 5,500,000 psi — Medium 580-690 psi	Y = 6" CRCP: 5,500,000 psi — High 690 psi(+)	Line
Poor 5.5+	Non-Stabilized	Fine Grain			XY			XX		1
		Crushed Stone			XX			X	X	2
	Stabilized	Cement			X	X		XXY	XY	3
		Asphalt			XY	X		X		4
		Lime		X	X					5
Fair 5.0–5.5	Non-Stabilized	Fine Grain			X			X		6
		Crushed Stone			X	X				7
	Stabilized	Cement						XX		8
		Asphalt			X			X		9
		Lime			X					10
Good 4.0–5.0	Non-Stabilized	Fine Grain			X			XXX		11
		Crushed Stone			X			X	X	12
	Stabilized	Cement			X			XXXY	XY	13
		Asphalt			X					14
		Lime			XY			X		15
Column				1	2	3	4	5	6	

Figure 1. Experiment design for continuously reinforced concrete pavement.

Subgrade Support	Subbase Type	Subbase Material	Modulus of Elasticity Concrete Flexural Strength	J8 = 8" Slab, 3,500,000 psi: Low 580 psi (–)	J8 = 8" Slab, 3,500,000 psi: Medium 580-690 psi	J8 = 8" Slab, 3,500,000 psi: High 690 psi (+)	J9 = 9" Slab, 5,500,000 psi: Low 580 psi (–)	J10 = 10" Slab, 5,500,000 psi: Medium 580-690 psi	J10 = 10" Slab, 5,500,000 psi: High 690 psi (+)	Line
Poor 5.5 +	Non-Stabilized	Fine Grain			J10					1
		Crushed Stone			J9, J10			J8, J9, J10		2
	Stabilized	Cement								3
		Asphalt								4
		Lime			J9, J10					5
Fair 5.0 – 5.5	Non-Stabilized	Fine Grain						J8		6
		Crushed Stone			J10			J8, J9, J10		7
	Stabilized	Cement								8
		Asphalt								9
		Lime			J10					10
Good 4.0 – 5.0	Non-Stabilized	Fine Grain			J10			J9		11
		Crushed Stone			J9, J10			J8, J9		12
	Stabilized	Cement						J9, J10		13
		Asphalt								14
		Lime								15
Column				1	2	3	4	5	6	

Figure 2. Experiment design for jointed concrete pavement.

experiment design in shown in Figure 1. In order to represent each entry in the factorial design for one pavement thickness, 90 different test sections would be required. Figure 1 shows the entries in the factorial table that were filled. Each symbol represents a test section; therefore, small degree of replication was provided for. It was quite impossible to fully complete the table due to the closely standardized design criteria. In this report the test sections will sometimes be referred to by number; e.g., 1-6 means line 1, column 6 on the factorial.

The variables represented in the factorial are the controlled variables—the subgrade support, subbase type, concrete modulus of elasticity, and concrete modulus of rupture. Similar charts were prepared for pavement thickness. Figure 2 shows the jointed pavement test sections in factorial arrangement.

Controlled Variables

In this experiment each level of the subgrade support variable was grouped in accordance with the Texas Triaxial Classification Chart (9, 10). For this factorial, the subgrades were classified as poor, fair, and good. Only the strength parameter was used for classifying the subgrade support variable, with no attempt to further subdivide with index properties such as sand, clay, grading, plasticity, etc. For each of these classifications, the triaxial class range was as follows:

Poor:	Class	5.5	and	above
Fair:	Class	5.0	through	5.4
Good:	Class	4.0	through	4.9

(In the Texas Triaxial Classification Chart, the numbers range from Class 1.0 to Class 6.0(+). The larger the number the weaker the material.)

The subbase was categorized in two general divisions, stabilized or unstabilized. Unstabilized subbases were subdivided into two basic categories, those with fine-grain materials (natural sands) and granular material. The stabilized subbases were either lime-, cement-, or asphalt-treated base material. As was the case with subgrade support, further subdivision in accordance with index properties was not considered. Therefore, a cement-stabilized material may be an iron gravel, crushed limestone, a sand shell, etc. The subbases were generally constructed in accordance with the Standard Specifications of the Texas Highway Department (11).

The modulus of elasticity (tangent modulus of elasticity) of the concrete pavement was based on the type of coarse aggregate used. In Texas, experience indicates that concretes with siliceous river gravel coarse aggregate exhibit a modulus of elasticity of about 5.5 million psi, whereas concretes with crushed limestone aggregate have a lower modulus of about 3.5 million psi. Thus it was on this basis of coarse aggregate source within the state that the modulus of elasticity of each pavement section was selected.

The modulus of rupture was divided into three categories—low, medium and high—representing concrete flexural strength ranges of less than 580, 580 to 690, and above 690 psi respectively (modulus of rupture obtained with mid-point loading). Each of the modulus of elasticity levels was subdivided into these three levels of modulus of rupture. Most of the pavement sections entered in the factorial were in the medium range, which is considered the optimum strength for CRCP.

Pavement thickness, also a controlled variable, could not be investigated to the extent desired because most of the CRCP in Texas is 8 in. thick. There has been some 6-in. CRCP built, but in a limited number of designs. Thus, it has been quite difficult to truly examine pavements with a lesser thickness than 8 in. Two different symbols are used in Figure 1 to represent the two pavement thicknesses considered.

Figure 2 shows the jointed pavement test sections. The three thicknesses are represented by symbols indicating the slab thickness. The sections represented in column 2 of Figure 2 are plain concrete and the sections in column 5 are reinforced. The load transfer at the transverse joints was by mechanical devices. This made it possible to make direct comparisons between jointed and continuous pavement. Everything was held constant in the factorial comparison except the pavement type.

Semi-Controlled Variables

Two other variables that were given due consideration but are not shown on the factorial in Figure 1 are the season of the year and the general soil moisture condition. The field data were taken in such a manner that all pavement test sections were studied in each of the four seasons of the year. The second semi-controlled variable was the general moisture condition of the soil, which is somewhat a function of the season. Data taken in winter and spring were in general taken under wet conditions, the spring being more so. The data taken in summer and fall were taken under generally dry conditions.

Another parameter considered to be constant was the subbase thickness, which was generally 6 in. ±2 in. Studies at the AASHO Road Test found that subbase thickness has very little effect on pavement deflection in the range of 3 to 9 in. (5). Therefore, the assumption of equal thickness is reasonable for the range of thickness considered, i.e., 4 to 8 in. The cement factor for the concrete pavement is generally $4\frac{1}{2}$ sacks per cubic yard. The longitudinal reinforcement for the pavement was approximately 0.5 percent in all cases.

Pavement Test Sections

The pavement sections used for test sections were essentially made up of three parts: the test section, the transition area, and the replicate test section. The test section and the replicate test section are both 1200 ft long and separated by a 100-ft transition area (Fig. 3). Jointed concrete pavement test sections were laid out the same as the CRCP.

West of the Balcones Fault Zone through central Texas, generally all pavements are flexible due to a combination of traffic density and availability of high-grade flexible

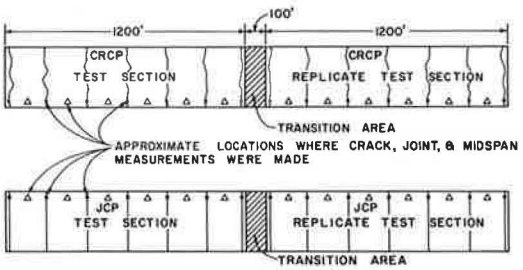

Figure 3. Layout of test pavements.

base construction materials. Consequently, the pavement test sections for this experiment were scattered throughout the eastern half of the state. Some of the criteria used in choosing the test sections were as follows:

1. The entire test section should be in a 2500-ft long tangent section with no grade in excess of 1 percent.
2. Longitudinal reinforcement should be approximately 0.5 percent steel.
3. The general soil conditions should be relatively constant as far as could be ascertained by engineering judgment and inspection.
4. The entire length, 2500 ft, when in cut or fill sections should be entirely therein to attain uniformity.
5. The structural components of the pavement must classify it into one of the 90 entries in the chart in Figure 1.
6. In no case were side-hill sections chosen for test sections.
7. The subbase must extend the entire crown-width of the roadway; trench-type sections were not considered.

Table 2 gives a brief description of materials components, location, traffic applications, etc., of the pavement test sections studied in this experiment.

METHOD OF ANALYSIS AND ACCURACY

The voluminous amount of data taken in this experiment required a careful and detailed analysis to obtain the desired end product. The 1604-A Control Data Computer was used to facilitate the analysis of the data to the greatest extent possible.

The computer program for the data reduction was written in such a fashion that all the pertinent data gathered would be presented for analysis. All data taken in the field were recorded on a data sheet, from which the data were key-punched, then processed, stored permanently on magnetic tape, and printed out. The print-out included the following: the pavement depth, identification of the test section, average crack spacing, general moisture condition of the soil, deflection data, crack width data, radius of curvature data, temperature data, and a statistical analysis of the temperature, deflection, radius of curvature, and crack width data. Also included on the computer print-out were the average deflections corrected to a zero degree temperature differential (6).

It should be emphasized here that each data point used in the following discussions and analysis represents the average of numerous readings. For each type of data point, the magnitude used to represent a test section was derived from an average of at least 14 data points.

Method of Analysis

The data were analyzed by investigating one variable at a time, i.e., holding all others constant. By using this method, it was possible to determine if the variable being studied was truly a variable or not. This method of having all but one variable constant in a comparison was made possible by the factorial design (Fig. 2). For example, in comparing subgrade support, any factorial entry under "poor" could be compared with a corresponding entry under "fair" or "good." This comparison would be clean, i.e., the subgrade support would be the only variable. This same procedure was used to investigate each variable under consideration in this study. Analysis of variance techniques were used on several of the parameters; however, not enough entries were filled in the factorial to validate the analysis of variance results, even though some trends were shown.

TABLE 2

DESCRIPTIVE INFORMATION RELATIVE TO SUBBASE AND SUBGRADE FOR THE TEST SECTIONS

Fractorial Number Line-Column	Test Section Number	County	Highway	Subbase				Subgrade			Remarks[a]
				Type	Triaxial Class	Unconfined Compressive Strength[b]	Stabilization	Type	Triaxial Classification[c]	Stabilization	
1-2	8-13-1	Tarrant	IH 820	Dark brown sand	1.0	117	6% Lime	Black clay	5.5	5% Lime	6-in. CRCP
1-2	8-13-2	Tarrant	IH 820	Dark brown sand	1.0	117	6% Lime	Shaley clay	5.5	5% Lime	
1-5	675-7-1	Walker	IH 45	Crushed sandstone	2.2	16.1	None	Sandy clay	5.5 (1.0)	3% Lime	
1-5	675-7-2	Walker	IH 45	Crushed sandstone	2.2	16.1	None	Sandy clay	5.5 (1.0)	3% Lime	
2-2	95-4-1	Kaufman	IH 20	Crushed limestone	1.0	50	None	Taylor marl	5.5 (1.0)	4% Lime	
2-2	94-7-1	Dallas	SH 183	River gravel	3.5	15.0	None	Del borrow	5.5	None	
2-5	739-2-4	Jefferson	IH 10	6 in. Sand-shell	2.0	65	None	Clay	6.0 (1.0)	4% Lime	
2-6	15-2-1	McLennan	IH 35	4 in. Bosque gravel	3.4	20.9	None	Silty clay	5.5 (1.0)	6% Lime	
3-2	739-2-7	Jefferson	IH 10	6 in. Sand-shell	1.0	600	7.1% Cement	Clay	6.0 (1.0)	4% Lime	
3-3	156-7-1	Wichita	US 277	4 in. Sandstone	1.0	270	3.0% Cement	Clay	5.5	None	
3-5	739-2-2	Jefferson	IH 10	6 in. Sand-shell	1.0	600	7.1% Cement	Clay	5.9 (1.0)	4% Lime	
3-5	500-3-3	Harris	IH 45	6 in. Sand-shell	1.0	1100	7.0% Cement	Silty clay	5.8	None	
3-6	27-13-1	Harris	US 59	6 in. Sand-shell	1.0	1100	7.0% Cement	Silty clay	5.6	None	
4-2	675-6-1	Walker	IH 45	4 in. Bituminous concrete (crushed sandstone)	1.0	226	5% OA-90 Asphalt	Sandy clay	5.5 (1.0)	3% Lime	
4-3	156-7-2	Wichita	US 277	Sandstone	2.7	28	Asphalt	Clay	5.5	None	
4-5	495-10-1	Harrison	IH 20	6 in. Sandy clay		30	Asphalt	Silty clay	5.5	None	
5-1	14-16-2	Tarrant	IH 35	6 in. Clay	1.0	100	5% Lime	Clay	5.5	None	
5-2	8-13-3	Tarrant	IH 820	6 in. Lime-treated subgrade	1.0	115	None	Dark brown clay	5.5	None	
6-2	14-16-1	Tarrant	IH 35W	Red sand-gravel	3.5	–	None	Black clay	5.7	None	
6-5	495-4-2	Smith	IH 20	Natural soil	4.0	6.5	None	Sandy clay	5.0	None	
7-2	17-10-1	Bexar	IH 35	Crushed limestone	1.0	41.0	None	Clay	5.5	3.5% Lime	
7-3	16-5-1	Comal	IH 35	Crushed limestone	1.0	–	5% Lime	Clay	5.6	None	
8-5	500-3-2	Harris	IH 45	6 in. Sand-shell	1.0	1100	7% Cement	Silty clay	5.2	None	
8-5	739-2-1	Jefferson	IH 10	6 in. Sand-shell	1.0	600	7.1% Cement	Clay	5.2 (1.0)	4% Lime	
9-2	675-6-2	Walker	IH 45	4 in. Bituminous concrete	1.0	226	5% OA-90 Asphalt	Sandy clay	5.2 (1.0)	3% Lime	
9-5	495-10-2	Harrison	IH 20	6 in. Sandy clay		30	Asphalt	Sandy clay	4.5	None	
10-2	442-2-1	Dallas	US 67	River gravel	2.0	15.0	3% Lime	Del borrow	5.2	None	
11-2	495-4-3	Smith	IH 20	Foundation course	3.5	16.9	None	Sandy clay	4.0	None	
11-5	495-4-1	Smith	IH 20	Foundation course	4.0	6.5	None	Sandy clay	4.0	None	
11-5	675-7-3	Walker	IH 45	Crushed stone	2.2	16.1	None	Sandy clay	4.6 (1.0)	3% Lime	
12-2	9-11-1	Dallas	IH 20	River gravel	3.5	15	None		4.0	None	
12-5	739-2-5	Jefferson	IH 10	6 in. Sand-shell	2.0	65	None	Clay	4.5 (1.0)	4% Lime	
12-6	15-2-2	McLennan	IH 35	Austin chalk	3.4	20.9	None	Silty clay	4.5 (1.0)	6% Lime	
13-2	739-2-6	Jefferson	IH 10	6 in. Sand-shell	1.0	600	7.1% Cement	Clay	4.5 (1.0)	4% Lime	
13-5	271-14-3	Harris	IH 610	6 in. Sand-shell	1.0	1100	7.0% Cement	Sandy clay	4.8	None	
13-5	535-8-1	Colorado	IH 10	Sand	1.0	492	4% Cement	Silty clay	4.6	None	
13-5	610-7-2	Bowie	IH 30	8 in. Sandy clay	1.0	315	Cement	Sandy clay	4.5	None	
13-6	271-14-1	Harris	IH 610	6 in. Sand-shell	1.0	1100	7.0% Cement	Sandy clay	4.8	None	
14-2	675-6-3	Walker	IH 45	4 in. Bituminous concrete	1.0	226	5% OA-90 Asphalt	Sandy clay	4.5 (1.0)	3% Lime	
15-2	8-13-4	Tarrant	IH 820	Shaley clay	1.0	100	5% Lime	Shaley clay	4.5	None	
15-5	610-7-1	Bowie	IH 30	6 in. Clay gravel	1.0	175	Lime	Sandy clay	4.5	None	
12-2	9-11-2	Dallas	IH 20	River gravel	1.0	114	3% Lime		4.0	None	
15-2	581-1-1	Dallas	Loop 12	River gravel	1.0	70	3% Lime	Houston clay	4.5 (1.0)	4% Lime	6-in. CRCP
2-2	14-16-3	Tarrant	IH 35N	6 in. Flexible base	3.5	–	None	Clay, rocky	5.5	Mechanical	
2-2	1068-1-1	Tarrant	IH 20	6 in. Flexible base	3.0	–	None	Clay, rocky	5.5	Mechanical	
11-5	675-7-4	Walker	IH 45	Crushed sandstone	2.2	16.1	None	Sandy clay	4.6 (1.0)	3% Lime	

[a]Unless specified otherwise in the "Remarks" column all pavements are 8-in. CRCP.

[b]Unconfined compressive strength at an age of 7 days tested in accordance with THD procedures.

[c]Classifications in parentheses are after addition of lime to subgrade material.

TABLE 3

STANDARD ERROR OF THE MEAN—DEFLECTION AND RADIUS OF CURVATURE

Data Run No.	Deflection		Radius of Curvature	
	Crack	Midspan	Crack	Midspan
1	0.000904	0.000911	541	1193
2	0.000818	0.000766	586	935
3	0.000785	0.000781	583	861
4	0.000647	0.000675	1013	1172

Accuracy of Data

In order to qualify the data, it was necessary to compare the accuracy of the measurements by type and position within each test section. The likeness of the data taken from pavement sections of identical design located throughout the state indicates quality data and good experimental technique. The following analyses were made to obtain a measure of the accuracy within a test section and a measure of the accuracy between replicate test sections in the same factorial entry.

Replication Within Test Section—For each individual test section, the standard error of the mean was calculated for deflection and radius of curvature measurements taken at both the crack and midspan positions. The average of these respective measurements was then calculated for each of the four individual runs; the results are given in Table 3. The error within a section presented here is well within the measuring accuracy of the equipment used. The deflection replication within a section is less than 0.001 in. in all cases; this magnitude is considerably less than the resolution of the Benkelman beam (±0.002 in.) (12). The standard errors for the radius of curvature measurements are somewhat larger than the resolution (80 ft) or replication error (250 ft) of the Basin beam (6).

Replication Between Test Sections—To determine the error between equivalent test sections, the standard error of the mean for the test sections within a given factorial block was determined. Only factorial blocks that had replicate sections were used in this analysis, and the number of replicate sections varied from one to two. It should be pointed out that these replicate sections were sometimes in different geographical areas of the state, such as Houston and Tyler. After determining the standard error of the mean for each of the applicable factorial blocks, these values were then averaged for the four data runs. The standard errors found were as follows:

Deflection:

$$\text{Crack position} = \pm 0.00172 \text{ in.}$$
$$\text{Midspan position} = \pm 0.00127 \text{ in.}$$

Radius of curvature:

$$\text{Crack position} = \pm 1525 \text{ ft}$$
$$\text{Midspan position} = \pm 2079 \text{ ft}$$

These results indicate that the error for the data in any factorial block did not significantly exceed the measuring capability of the equipment used. Furthermore, the small error lends credence to assumptions that the test sections were properly classified in the factorial design for this experiment.

ANALYSIS OF DATA

In this section, the data analysis is presented in such a manner that one variable is studied at a time. The radius of curvature data were converted to stress by simple calculation and analyzed in terms of stress rather than the field measurement of radius of curvature. This method of conversion was covered in a previous report on this project (6). The data are presented in bar graph fashion, weighted relative to the total for any type of measurement so that the sum of the four runs is equal to 100 percent.

Controlled Variables

The controlled variables, as previously defined, are the first to be considered in this analysis. The controlled variables are broken into the categories of support properties, concrete properties, and slab thickness and type.

Support Properties—The strength property of the subgrade and its effect on deflection and stress at the crack and midspan position is investigated by comparing data from test sections that were identical except for the subgrade. These comparable sections were taken from the factorial. The weaker subgrade was evaluated in comparison with the better subgrade. There are three basic comparisons for each of the identical sections (except for subbase), i. e., poor to fair, poor to good, and fair to good. The comparisons were made by season or data run and by the total for the four seasons.

Figure 4 shows how the subgrade affected deflection in terms of the percent of the comparisons made. In each of the four seasons the pavements on the weaker subgrade deflected more than comparable pavements on better subgrades. Considering the total comparison, the weaker subgrade deflected more than the better subgrade in 67 percent of the comparisons.

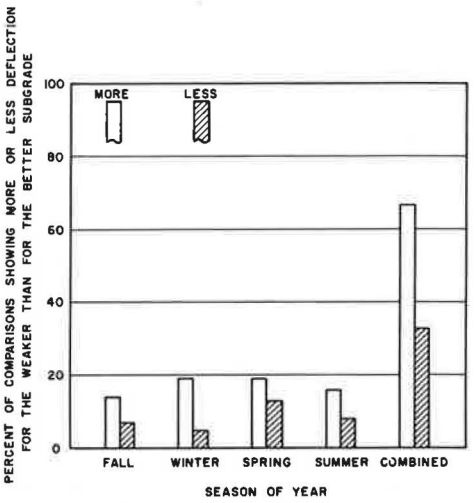

Figure 4. Deflection comparison of a weaker subgrade with a better subgrade.

Figure 5 shows how the subgrade affected concrete pavement stress in terms of the percent of comparisons made. As was the case with deflection, the pavement with the weaker subgrade experienced more stress than one with a better subgrade 60 percent of the time. In all four seasons the pavement with the weak subgrade generally had more stress than one with a better subgrade.

Inspection of Figures 4 and 5 indicates that deflection and stress are directly related to the subgrade support quality, i. e., the better the subgrade, the less deflection and stress there will be. The results for each season indicate this trend. It has been shown that CRCP with poor subgrade deflected 19 and 25 percent more on the average than CRCP with fair and good subgrade respectively. Also pavement with a fair subgrade deflected 9 percent more on the average than did the pavement with the good subgrade.

Calculations show that the CRCP with the poor subgrade had approximately the same stress as did the one with the fair subgrade; however, the pavements with the good subgrade had 15 percent less stress than the CRCP with the poor subgrade.

The subbases that were included in this study were evaluated on a comparative basis with all other variables constant. The deflection of a test section was compared with the deflection on all other types of subbases on the same subgrade class. The results for each subbase type were evaluated for each of the four seasonal data runs. The results for each season followed the same general trend. Figure 6 compares the subbases in terms of deflection on a percentage of comparisons basis (compilation of all four runs). The stabilized subbases appear to be superior to the non-stabilized materials as far as deflection is concerned. The stress analysis showed the same trends with respect to the subbase characteristic (Fig. 7).

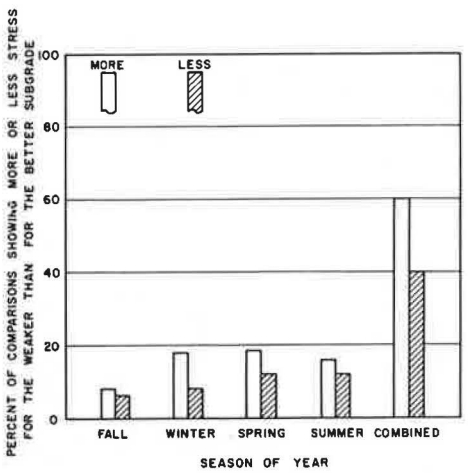

Figure 5. Stress comparison of a weaker subgrade with a better subgrade.

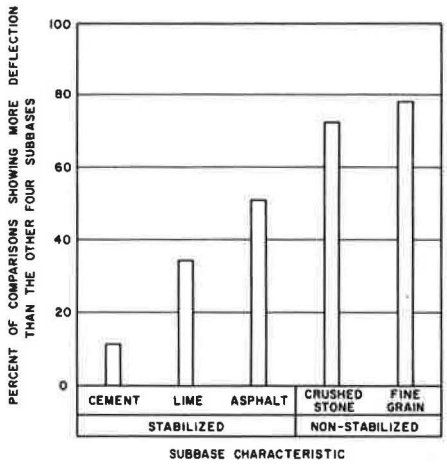

Figure 6. Deflection comparison of each subbase with the other four types.

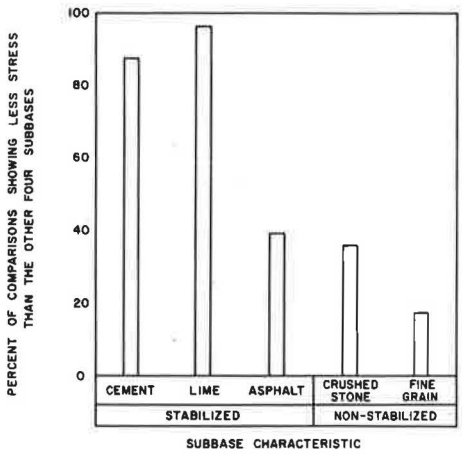

Figure 7. Stress comparison of each subbase with the other four types.

Concrete Properties—The two properties of the concrete that are part of this analysis are the modulus of elasticity and the modulus of rupture or flexural strength. The modulus of elasticity was determined from the type of coarse aggregate in the concrete. Concrete with siliceous river gravel is referred to as high modulus and that with crushed stone is referred to as low modulus of elasticity concrete. In Figure 8, for each data run and all runs combined the deflection is compared on the low and high modulus concrete. On the ordinate the percent of comparisons is plotted in which the low modulus of elasticity concrete deflected more or less than the high modulus of elasticity concrete. For each season except fall the graph has two entries. The cross-hatched bar shows the percent of comparisons made in which the low modulus of elasticty concrete deflected less than the high and the plain bar indicates the comparisons in which low

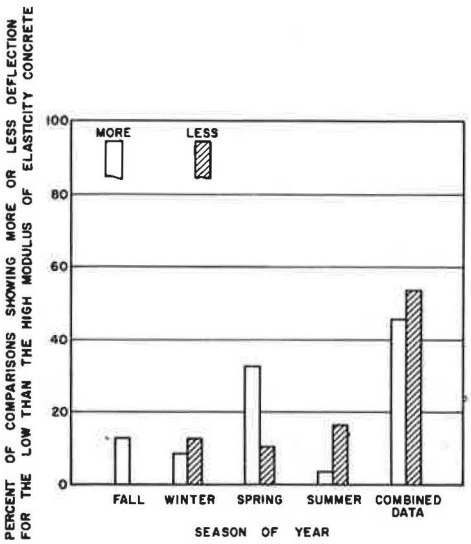

Figure 8. Deflection comparison of low and high modulus of elasticity CRCP.

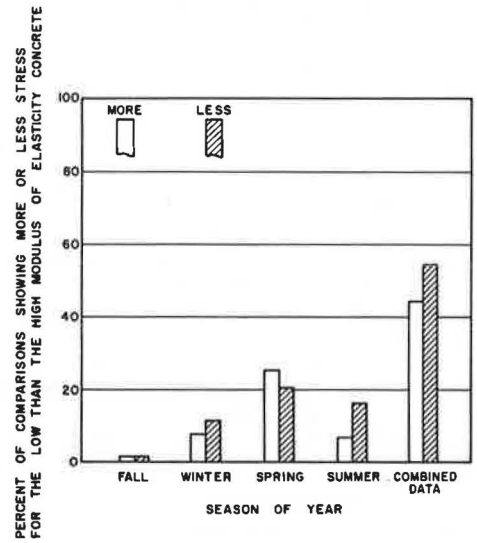

Figure 9. Stress comparison of low and high modulus of elasticity CRCP.

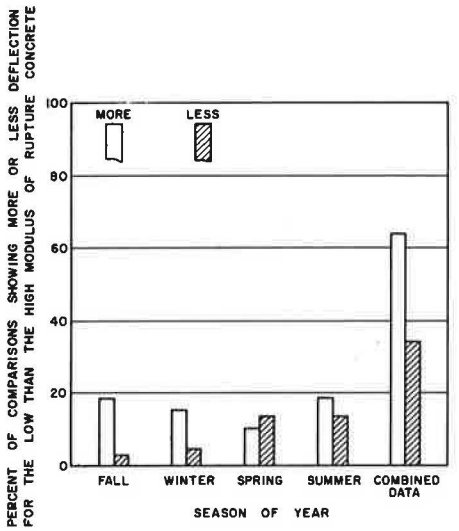

Figure 10. Deflection comparison of low and high modulus of rupture concrete.

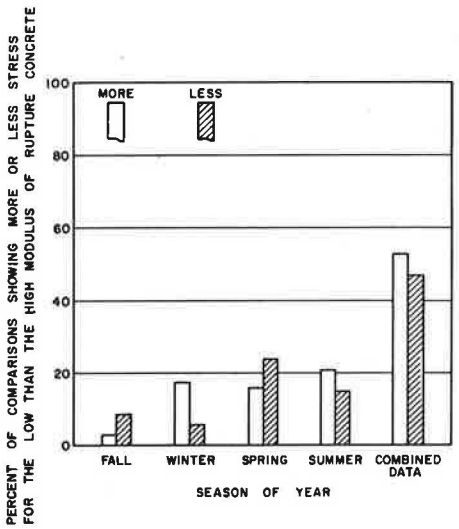

Figure 11. Stress comparison of low and high modulus of rupture concrete.

modulus deflected more than the high modulus of elasticity concrete. The range of modulus of elasticity experiencing the most deflection apparently varies slightly with season. Calculations have shown that, on the average, the lower modulus of elasticity concrete in general deflected 7.4 percent less than the high modulus of elasticity concrete. This finding, although contrary to rational reasoning, is in line with that found in another experiment (7).

Figure 9 is bar graph comparing modulus of elasticity against stress in the concrete slab. The graph structurally is the same as Figure 8 except that it portrays stress in the concrete. Inspection of Figure 9 shows that more comparisons of stress on low and high modulus of elasticity concrete showed less stress in the low than the high modulus concrete. The range of modulus of elasticity experiencing the most stress also varies with season.

The second concrete property considered here is the modulus of rupture. The analysis of the modulus of rupture was made by determining whether the deflections and stresses were more or less for the lower modulus of rupture concrete than the higher modulus of rupture CRCP. The evaluation was made for each season and also the combined data. Figure 10 shows in bar graph style the percentage of comparisons in which deflections on the high modulus of rupture concrete were more or less than those on the low modulus of rupture concrete. Note that the low modulus of rupture concrete deflects more than does the high. This was true for all seasons except for the spring. The combined data also show that the average deflection for all seasons is greater on the low modulus of rupture concrete.

The comparison of stresses on the low and high modulus of elasticity concrete indicate that, on the average, stresses were higher in the low than the high modulus of rupture concrete. Figure 11 shows the percent of comparisons in which the stress was higher or lower than that in the low modulus of rupture concrete.

Slab Thickness and Type—The pavement slab thickness analysis was made by comparing deflection measurements from sections that had identical classifications in the factorial, but different slab thickness. This allows a clean comparison of thickness to deflection and stress.

In each case the smaller thickness of concrete pavement was compared with a greater thickness. The results were combined for all four data runs. The comparison may not be very good because of the small number of sections compared.

TABLE 4

PERFORMANCE OF RIGID PAVEMENT IN TERMS OF THICKNESS, PAVEMENT TYPE, AND LOAD POSITION*

Thickness Comparison	Deflection		Stress	
	Crack or Joint	Midspan	Crack or Joint	Midspan
6-in. CRCP vs 8-in. CRCP	41.1	54.6	11.0	1.1
8-in. CRCP vs 9-in. JCP	-13.1	30.8	-50.2	-11.1
8-in. CRCP vs 10-in. JCP	-38.0	-28.5	-49.6	6.9

*Numbers indicate the average percent difference for the respective condition.

Table 4 is a summary of the results obtained in comparing pavements of different thickness and type. In comparing 6-in. CRCP with 8-in. CRCP, it was found that the 6-in. pavement deflected 41 percent more at the crack position than did the 8-in. CRCP. Comparing 8-in. CRCP with 9-in. JCP, it was found that the CRCP deflected on an average of 13.1 percent less than the JCP. When the 8-in. CRCP was compared to 10-in. JCP, it was found that the CRCP deflected on an average of 38 percent less than the 10-in. JCP.

It has been assumed in the past that 10-in. JCP performance would be very much the same as that of 8-in. CRCP (4). Performance measured in terms of deflection shows that the 8-in. CRCP is superior to the 10-in. JCP. In Figure 12 deflections as computed by the equations developed herein are plotted against deflections measured on comparable 10-in. JCP. The deflections for both pavement types have been corrected to zero temperature differential, and the deflections for CRCP were corrected to an 8-ft crack spacing and a 0.014-in. crack width. The data show a remarkable relation between the two parameters. By forcing the correlation line through zero (a rational approach), the slope of the line indicates that a 10-in. JCP deflects 1.6 times more than an 8-in. CRCP.

Deflection Position—On each test section a midspan deflection (between cracks) was obtained each time a reading was taken at the crack position. Figures 13 through 16 are plots of the average crack deflection versus the midspan deflection for each of the four runs. Although there is an offset on the vertical axis (crack deflection) greater than zero, it may be stated that the edge deflection and crack deflection are approximately equal on any range of support properties with continuous pavements that have 0.5 percent longitudinal steel or greater.

The radius of curvature measurements were also plotted in the same manner as deflection measurements (Figs. 17 through 20). In the case of radius of curvature—in contrast to deflection—the crack position has considerably less magnitude than the midspan position, which means that the concrete at the crack position is experiencing considerably more stress.

In terms of deflection and radius of curvature, it is evident that the aggregate interlock produces adequate load transfer across a crack, but the transverse cracks affect the continuity condition of the slab.

Semi-Controlled Variables

Two factors studied on a semi-controlled basis were the season of the year that the field measurements were taken and the general moisture condition of the soil.

Season—Data were taken on a statewide basis in each of the four seasons of the year. The deflection and radius of curvature data taken during these four seasons were analyzed by comparing each set of data with that taken during the summer. The comparison showed only whether the deflections and stresses were more or less in the fall, winter, and spring than in the summer. In Figure 21 these comparisons showing more or less deflection than the summer data are expressed as percentages. The results indicate that the deflections during fall and winter were generally greater than the summer, whereas the spring deflections were significantly smaller than the summer. Thus the

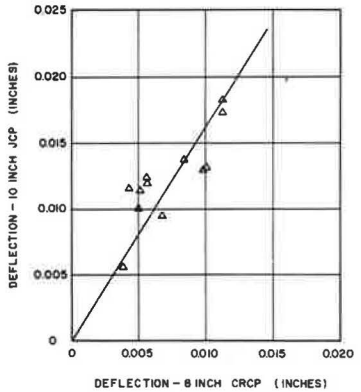

Figure 12. Calculated 8-in. CRCP deflection vs measured 10-in. JCP deflection.

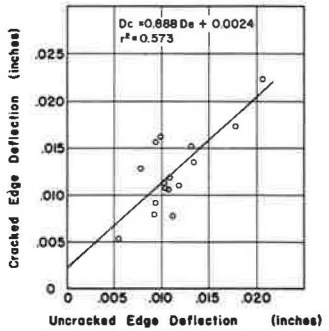

Figure 13. Cracked edge vs uncracked edge deflection—fall.

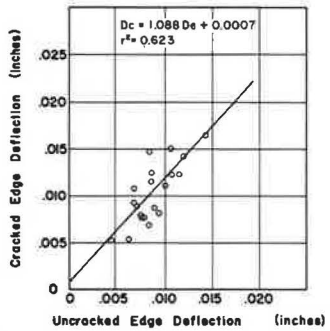

Figure 14. Cracked edge vs uncracked edge deflection—winter.

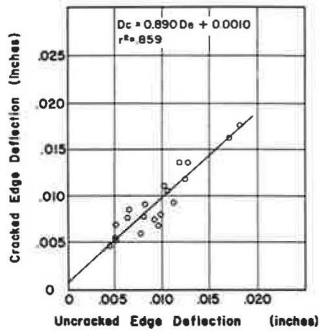

Figure 15. Cracked edge vs uncracked edge deflection—summer.

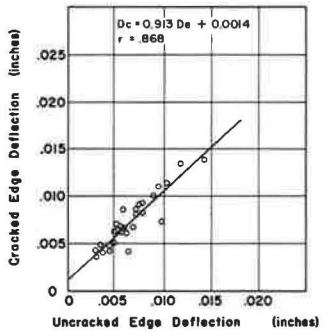

Figure 16. Cracked edge vs uncracked edge deflection—spring.

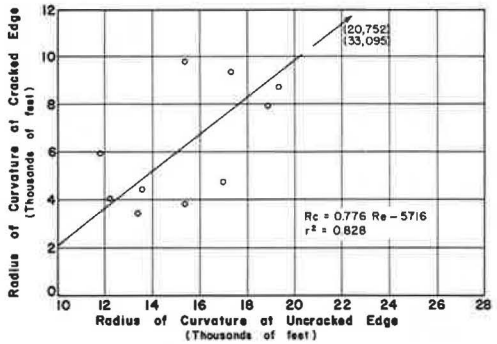

Figure 17. Cracked edge vs uncracked edge radius of curvature—fall.

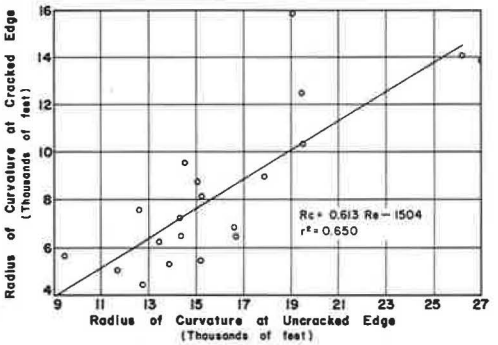

Figure 18. Cracked edge vs uncracked edge radius of curvature—winter.

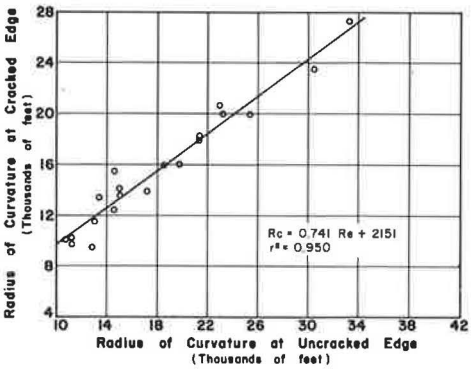

Figure 19. Cracked edge vs uncracked edge radius of curvature—summer.

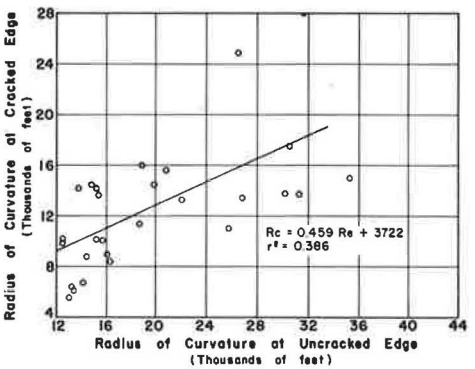

Figure 20. Cracked edge vs uncracked edge radius of curvature—spring.

deflection might in some way be related to the season; however, for the fall and winter there was not very much difference in the data.

The results of the stress analysis shown in Figure 22 indicate that the seasonal comparisons with the summer data are consistent in showing that the pavements experience less stress in the summer than during the other seasons.

Soil Moisture Condition—Each time data were taken on a test section, the general environmental conditions of the soil adjacent to the roadway in a hole 1 ft deep was classified as dry, moist, or wet. As far as the moisture effects are concerned, it was found that the fourth data run, which was the spring run, measured deflections that were much less. During the entire spring run general rains were experienced over the state. Of the four runs, the spring run was by far the wettest.

CORRELATION OF VARIABLES

Deflection

The variables studied that affect deflection are the crack spacing, surface crack width, concrete modulus of elasticity and modulus of rupture, pavement slab thickness, pavement type, strength characteristics of the subgrade and subbase, and moisture conditions. With the exception of the semi-controlled variables and the modulus of rupture, these variables will be correlated into an equation in the following.

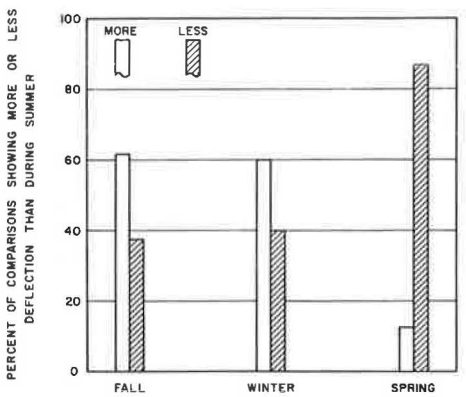

Figure 21. Seasonal comparison of deflection.

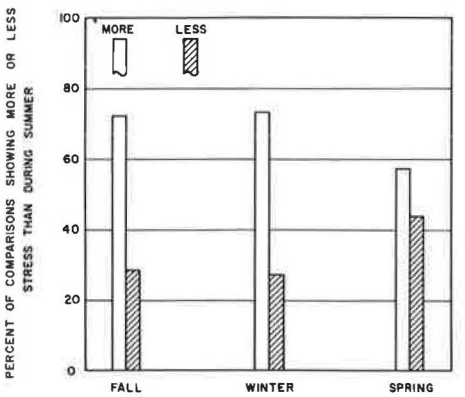

Figure 22. Seasonal comparison of stress.

A model equation was developed which encompassed the variables to be correlated. The model was based on previous work and also on work done at the AASHO Road Test (5, 8). The model chosen to relate the variables is basically an extension of the Road Test model and is of the following form:

$$D_C = \frac{A_0 \, L \, 10^{B_5} \, \Delta X \, \bar{X}^{B_4}}{D^{1.75} \, E^{B_2} \, SS^{B_3} \, 10^{0.0147 \, T}} \tag{1}$$

where

L = Load in kips;
X = Surface crack width in inches;
$\bar{X}$ = Average crack spacing in feet;
D = Slab thickness in inches;
E = Concrete modulus of elasticity, psi;
SS = Soil support;
D_C = Deflection at crack position, inches;
D_e = Deflection at midspan position, inches;
T = Temperature differential between top and bottom of the slab, degrees F; and
A_0, B_1, B_2, B_3, B_4, and B_5 are constants determined from a regression analysis on the data.

Slab thickness was not truly a full factorial variable, and consequently could not be entered as an independent variable and had to be analyzed separately. All the subsequent regression analyses were performed for the 8-in. pavement thickness factorial. The 1.75 power for the thickness term will be established later.

The soil support term is a combination of the subgrade and subbase strength characteristics. The soil support is a calculated value developed in a previous analysis. In some cases the natural soil was stabilized with lime (generally clay) to facilitate construction operations by providing a working platform.

The soil support is defined as

$$SS = \left(\frac{U_1 + U_2}{T_{sg}} \right) \tag{2}$$

where

SS = Soil support;
U = Unconfined compressive strength of subbase and subgrade materials in psi at an age of 7 days;
T_{sg} = Texas triaxial classification of subgrade material; and
1, 2 = Subscripts denoting subbase and stabilized subgrade respectively.

In all subsequent analysis the load, L, will be 18 kips and the pavement slab thickness will be 8 in. The linear form of load used here has been qualified in another report on this project (7) and in studies by others (5). The data from each run were carefully analyzed to screen out what might be considered erroneous.

The power term for the temperature differential term was derived in another report on this overall study (8). The temperature differential, the pavement thickness, and the load terms were not a part of the full factorial experiment, but in order that their effect would be reflected in the A_0 term, constant values for the 8-in. factorial were inserted into the equation for variables not considered in the semi-factorial experiment. The values inserted into the equation were an 18-kip single axle load, 8 in. for pavement thickness, and zero for temperature differential. These factors were then considered as constant and moved to the left of the equation.

A multiple regression analysis was made using the computer on each data run for deflection at the crack position, D_C, and also for deflection midway between cracks, D_e. The constants and the statistics derived from the regression analysis of each of the four runs are given in Table 5.

TABLE 5

COMPUTED CONSTANTS AND STATISTICS FROM REGRESSION ANALYSIS*

Load Position	Data Run No.	Computed Values							
		A_0	B_2	B_3	B_4	B_5	r	r^2	σ
Crack	1	6.664	0.334	0.681	-0.060	3.222	0.698	0.487	±0.0032
	2	0.00256	-0.123	0.526	0.1100	13.437	0.551	0.303	±0.0029
	3	0.1220	0.104	0.690	0.0900	13.911	0.662	0.438	±0.0030
	4	0.1099	0.1249	0.6869	0.0794	13.575	0.694	0.482	±0.0021
Midspan	1	0.0118	-0.0684	0.3211	-0.1938	7.816	0.407	0.166	±0.0035
	2	0.0726	0.0418	0.3434	-0.3294	7.055	0.244	0.060	±0.0032
	3	0.00373	-0.124	0.8709	0.1814	11.798	0.733	0.538	±0.0027
	4	0.0749	0.1026	0.7179	0.1897	4.876	0.515	0.265	±0.0031

*FOR EQUATION 1: r = coefficient of correlation, r^2 = coefficient of determination, σ = standard error of estimate.

The calculated deflection was plotted against the measured deflection for each data run and for each load position. These graphs are shown in Figures 23 through 30. Note the same general pattern for runs 1, 2, and 3 for both the crack and midspan deflections. The deflections at both crack and midspan were very small on run 4, as discussed previously, when compared with the three previous data runs.

In Table 5 note that several values of B_4 are negative. This same result was the case in a previous analysis (8). The crack spacing deflection relationship is a bowl-shaped curve, concave upwards. When the crack spacing is greater than that at the point of zero slope, B_4 is positive, and when it is smaller, B_4 is negative. Figure 31 is an example of the deflection-crack spacing relationship that results in a change of signs on B_4.

Several of the values calculated for B_2 are also negative. B_2 is the exponent on the modulus of elasticity term in the model equation. A negative B_2 would be in disagreement with theoretical concepts. Earlier it was pointed out that the low modulus of elasticity CRCP was deflecting less than the high modulus of elasticity CRCP. Another investigation on an experimental CRCP showed this same factor between lightweight and conventional aggregate concrete (7).

Note that the constants for each variable term generally have approximately the same magnitude, with only a few exceptions. The data from the first three runs were comparable, and therefore they were combined and a regression analysis was run. This resulted in two final equations, one for deflection at the crack position and another for deflection at a point midway between cracks. The computed constants and statistics are given in Table 6. The equation would be applicable to a dry condition; for a wet condition the equation for run 4 would be used. Note that the standard error is only slightly greater than the resolution of the Benkelman beam.

Radius of Curvature

The radius of curvature data have been examined thus far in terms of stress, but the subsequent analysis will be in terms of the radius of curvature data.

TABLE 6

COMPUTED CONSTANTS AND STATISTICS FOR DEFLECTION EQUATIONS

Load Position	Regression Analysis Computations							
	A_0	B_2	B_3	B_4	B_5	r	r^2	σ
Crack	0.3779	0.1683	0.6513	0.0266	6.3407	0.6971	0.486	±0.0028
Midspan	0.1362	0.0977	0.5601	-0.0462	4.1266	0.5544	0.307	±0.0033

Note: r = coefficient of correlation, r^2 = coefficient of determination, σ = standard error of estimate.

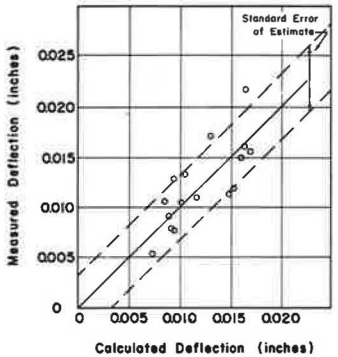

Figure 23. Measured vs calculated deflection at cracked edge—fall.

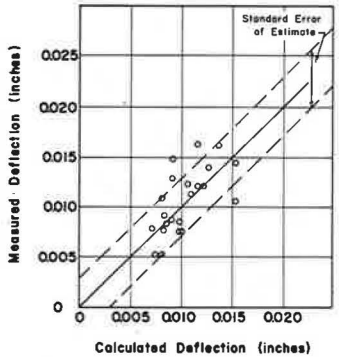

Figure 24. Measured vs calculated deflection at cracked edge—winter.

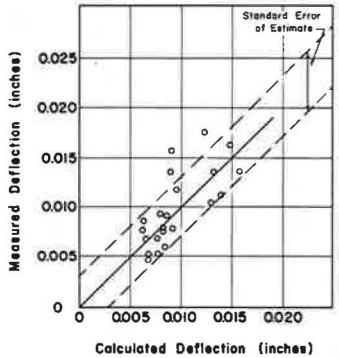

Figure 25. Measured vs calculated deflection at cracked edge—summer.

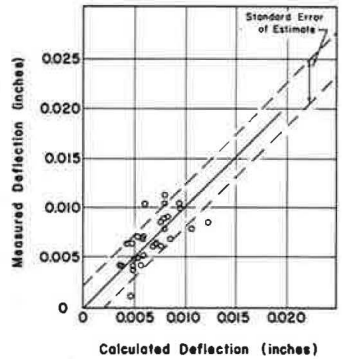

Figure 26. Measured vs calculated deflection at cracked edge—spring.

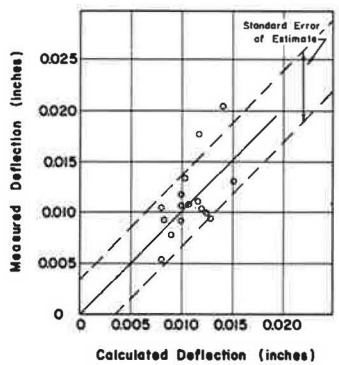

Figure 27. Measured vs calculated deflection at uncracked edge—fall.

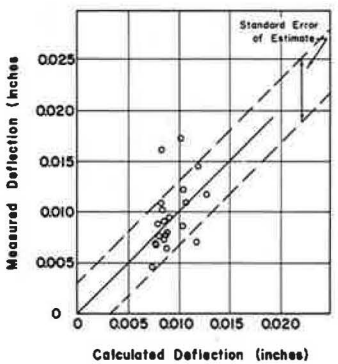

Figure 28. Measured vs calculated deflection at uncracked edge—winter.

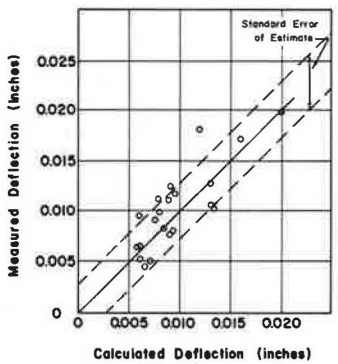

Figure 29. Measured vs calculated deflection at uncracked edge—summer.

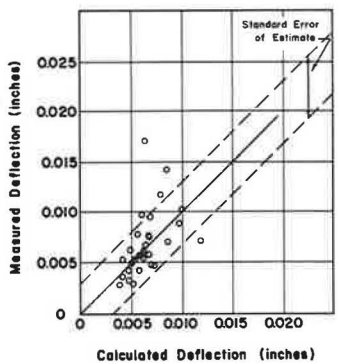

Figure 30. Measured vs calculated deflection at uncracked edge—spring.

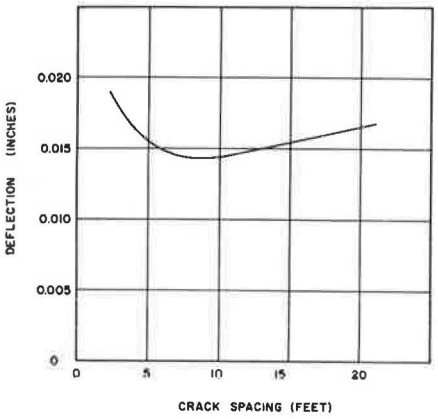

Figure 31. Deflection vs crack spacing.

The variables investigated that might affect the radius of curvature are the average crack spacing, soil support, concrete modulus of elasticity, load, and slab thickness. Thus, radius of curvature is some function of all these variables:

$$R_c,\ R_e = f(\overline{X},\ SS,\ E,\ L,\ D)$$

where

R_c = Radius of curvature at crack position, and

R_e = Radius of curvature at midspan position.

All other terms have been defined previously.

A model equation for radius of curvature was logically derived using the same concept as developed in the deflection equation. The following is the model with variables considered:

$$R_c = \frac{A_0\, D^{1.75}\, E^{B_2}\, SS^{B_3}\, \overline{X}^{B_4}}{L} \qquad (3)$$

All terms are as previously defined.

In the radius of curvature study the slab thickness again could not be entered as an independent variable because of a shortage of test sections on pavement thinner than 8 in. Thus the same thickness term was used here as in the deflection analysis, $D^{1.75}$.

Although the crack width and temperature differential are not reflected in Eq. 3, they were considered in this study and previous studies. Previous studies indicated that the effect of temperature differential on the radius of curvature was very slight or nonexistent. Therefore, on this basis, the temperature differential term was deleted. With regard to crack width, this term was included in the equation, but it was found that the statistics of correlation were improved by deleting it from the regression equation.

The radius of curvature of the CRCP is studied at two points on the continuous slab, across the volume change crack and midway between the cracks. The crack radius of curvature was analyzed for each data run except the fourth. The individual data runs were analyzed using multiple regression techniques. The regression constants for the model equation are given in Table 7. In order to obtain a more general equation for the radius of curvature at the crack position, the field data were examined and runs 1 and 2 were combined to form the data for the regression that would produce the final equation for radius of curvature at the crack position. Figures 32 through 35 show the measured radius of curvature plotted against the calculated radius of curvature for the crack position for runs 1, 2, and 3 and the combined data. The computed constants and the statistics for the final equation are given in Table 8.

TABLE 7

COMPUTED CONSTANTS AND STATISTICS FROM RADIUS OF CURVATURE ANALYSIS*

Load Position	Data Run No.	Computed Values						
		A_0	B_2	B_3	B_4	r	r^2	σ
Crack	1	0.000832	0.9819	0.6572	-0.2623	0.9518	0.9059	± 962
	2	350.5333	0.1548	0.3429	-0.1766	0.5574	0.3107	±1716
	3	53.4066	0.2898	0.4070	-0.0035	0.6900	0.4762	±2132
Midspan	1	0.0742	0.7395	0.1882	0.0277	0.9527	0.9076	± 868
	2	1779.2667	0.0639	0.3102	0.0863	0.4368	0.1908	±2247
	3	313.4298	0.1736	0.5872	0.0345	0.7503	0.5630	±2798
	4	1337.6603	0.0832	0.2894	0.1147	0.4453	0.1983	±2525

*FOR EQUATION 3: r = coefficient of correlation, r^2 = coefficient of determination, σ = standard error of estimate.

TABLE 8

COMPUTED CONSTANTS AND STATISTICS FOR RADIUS OF CURVATURE EQUATIONS

Load Position	Regression Analysis Computations						
	A_0	B_2	B_3	B_4	r	r^2	σ
Crack	15.3039	0.3312	0.5467	-0.0772	0.6391	0.4085	±1617
Midspan	333.3153	0.1729	0.3579	0.0909	0.5957	0.3548	±2508

Note: r = coefficient of correlation, r^2 = coefficient of determination, σ = standard error of estimate.

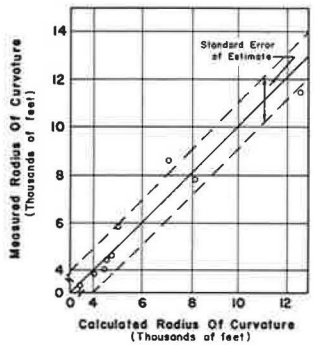

Figure 32. Measured vs calculated radius of curvature at cracked edge—fall.

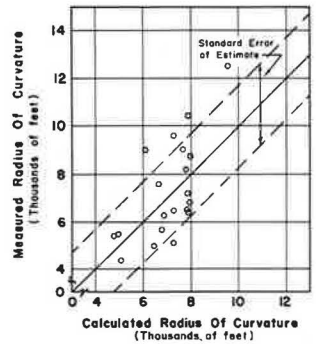

Figure 33. Measured vs calculated radius of curvature at cracked edge—winter.

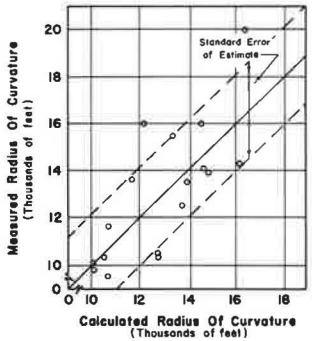

Figure 34. Measured vs calculated radius of curvature at cracked edge—summer.

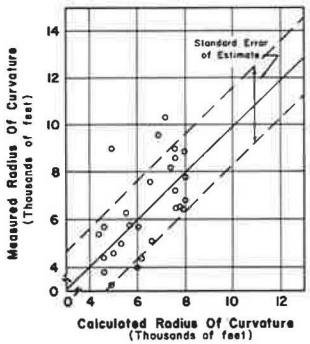

Figure 35. Measured vs calculated radius of curvature—combined data.

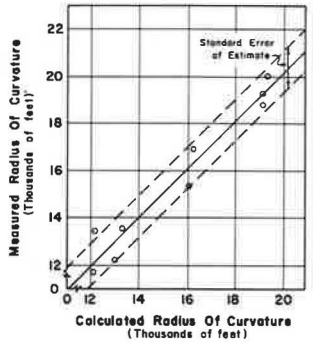

Figure 36. Measured vs calculated radius of curvature at uncracked edge—fall.

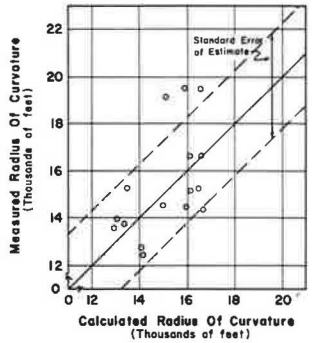

Figure 37. Measured vs calculated radius of curvature at uncracked edge—winter.

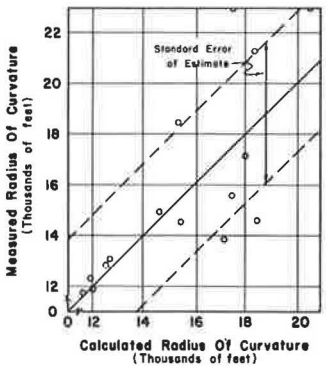

Figure 38. Measured vs calculated radius of curvature at uncracked edge—summer.

The midspan radius of curvature data were analyzed in like manner as the crack radius data; however, here all four data runs were used to relate the parameters studied to radius of curvature. The computed constants and statistics for the four equations are given in Table 8. Figures 36 through 39 show the calculated radius of curvature plotted against the measured midspan radius of curvature.

DISCUSSION OF RESULTS

Deflection

In general, the control variables considered in this study were found to affect the deflection of a CRCP. Their effect follows a pattern that can be expressed by a mathematical expression. Of the semi-controlled variables considered, it was found that the soil moisture condition affected the deflection, although the findings were contrary to the generally accepted criteria of greater deflection for a moist condition. In addition, the findings of this study tend to verify the assumptions used in the design and development of CRCP.

Soil Moisture—The four data runs were made in different seasons over a period of about two years. At the times the data were taken, the general soil moisture conditions were not the same. The fourth run was exceptionally wet, and deflections on this run were all considerably less than they had been on the first three runs. Initially, this discrepancy between the findings and the normal assumption of more deflection for a wet condition caused much concern for errors that might have been made on the fourth run in taking the data. When the weather conditions were the same as on the fourth run, the pavement deflections on approximately one-third of the sections were measured again. As was the case previously, the deflections were small and for all practical purposes identical to those of the fourth run.

It is now believed that when the subgrade and subbase materials are saturated they respond to quick loading as does a soil sample in an undrained triaxial test. The load applied to the pavement is supported partially by the pore water in the pavement foundation rather than the soil grains as is the case where the soil is not saturated (13).

It should also be pointed out that the summer run, where the soil was the dryest, experienced slightly less deflection than periods when the subsoil was partially saturated. Of course, this latter condition could be the result of smaller cracks due to summer temperatures.

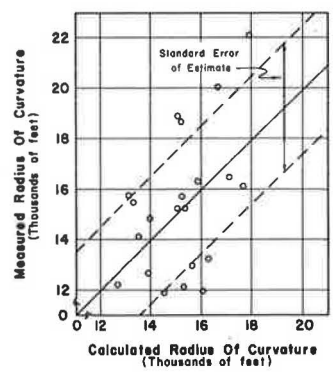

Figure 39. Measured vs calculated radius of curvature at uncracked edge—spring.

Equations—The deflection equations derived herein are extensions of the one developed in an earlier report (8). The previous equation was based on data taken from only two test sections, and those herein are based on 20 pavements with three sets of data from each for the dry condition and one set for the wet run. Table 9 gives a comparison of the equations with the equation developed earlier (8), which was based on crack position data only.

Figures 40 and 41 were prepared to illustrate the capability of the equation for predicting the observed deflection. In each case, the regression equation developed from the data for both the crack position and midspan position was used to calculate the deflection for a given set of conditions on a test section. This calculated deflection was then compared against measured deflections for the test sections as portrayed in the figures. Note the close

agreement, in most cases, between the measured and calculated values. In some cases, both the measured and calculated deflection appear to be out of line with what is to be expected, but these exceptions are normally due to a lime-stabilized subgrade and are so marked on the figures. These figures are typical of all runs, and hence, these observations support the validity of using these equations in design work.

TABLE 9

COMPARISON OF REGRESSION ANALYSIS CONSTANTS

Constant	Overnight Study	Statewide Study
A_0	0.0106	0.3779
B_2	—	0.1683
B_3	0.8503	0.6513
B_4	0.0994	0.0266
B_5	4.8997	6.3407

$$D_c = \frac{A_0 L 10^{B_5 \Delta X} \bar{X}^{B_4} T_{sg}^{0.25 B_3}}{D^{1.75} E^{B_2} U^{0.25 B_3} 10^{0.0147 T}}$$

Modulus of Elasticity—The findings in this study in regard to the modulus of elasticity of concrete contradict the generally accepted theory of a lower modulus of elasticity slab deflecting more than a high modulus one for equal conditions. Although the levels of the modulus are not too far apart in magnitude, another experiment on this same research project, wherein the levels were considerably greater through the use of two entirely different coarse aggregate types, indicated the same results. These two separate investigations, along with a limited laboratory investigation,

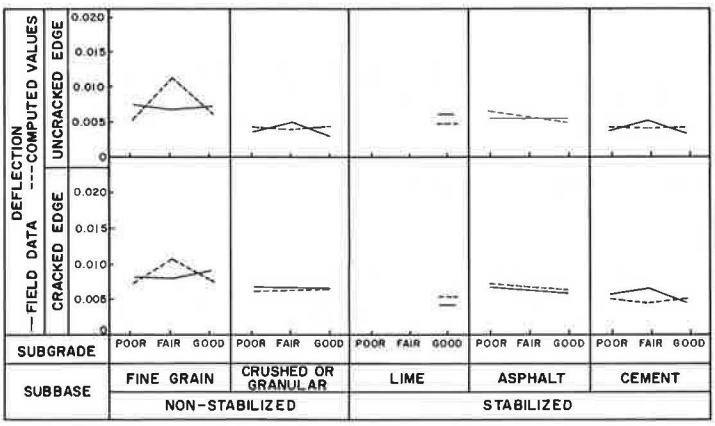

Figure 40. Measured and computed deflections on high modulus of elasticity concrete.

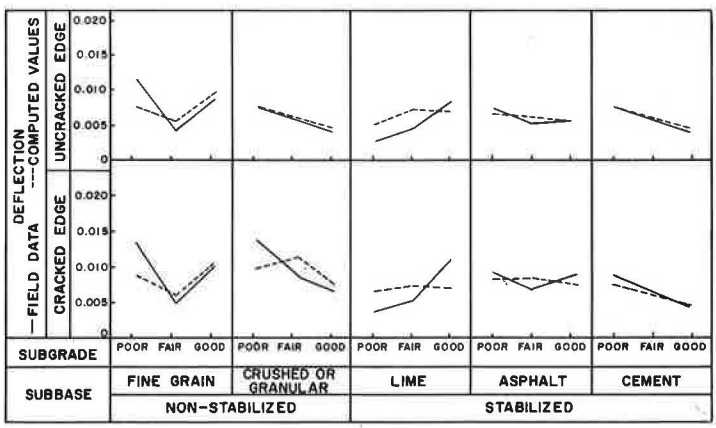

Figure 41. Measured and computed deflections on low modulus of elasticity concrete.

lend credence to the observations of less deflection with a lower modulus of elasticity concrete (14). It should be emphasized, however, that this observation can only be related to CRCP at this time and should not be translated to JCP, which may react differently.

There is a good possibility that this controversial observation attributed to modulus of elasticity could be an indirect effect of a combination of variables not considered in this experiment.

It may be hypothesized that generally speaking, a low modulus of elasticity concrete has a lower coefficient of thermal expansion. In this case the transverse volume change cracks would be smaller, and hence a greater degree of load transfer would be available. Therefore, with a greater load transfer less deflection would be experienced.

Furthermore, in the normal theoretical analyses of this condition, such as those of Westergaard, Pickett, Spangler, etc., the basic assumption is made that the subgrade reaction forces are vertical. An actual pavement on a subgrade deflecting under a wheel load develops a complicated interaction of shear forces and vertical forces, which may result in these field observations rather than those developed in a simplified theoretical approach.

Final Equation—The equations developed contain the term soil support, which was defined by Eq. 2. The soil support term can be eliminated from the deflection equations by substitution of Eq. 2 into Eq. 1. The dry or partially saturated condition was used as the level for selecting the final equation. Thus, the equation for deflection takes the form

$$D_c = \frac{0.3779\ L\ 10^{6.3407\ \Delta X\ \bar{X}^{0.0266}\ T_{sg}^{0.1628}}}{D^{1.75}\ E^{0.1683}\ (U_1 + U_2)^{0.1628}\ 10^{0.0147\ T}}$$

where all terms are as previously defined.

Radius of Curvature

The radius of curvature data show that the average radius of curvature at the cracked edge for all data is about 52 percent less than the radius of curvature at the uncracked edge. The radius of curvature at the crack and midspan was correlated by linear regression analysis for each of the four data runs, and the graphs were shown in Figures 17 through 20.

Figures 42 and 43 show calculated and measured radius of curvatures plotted against the subgrade classifications for each subbase material type that was available.

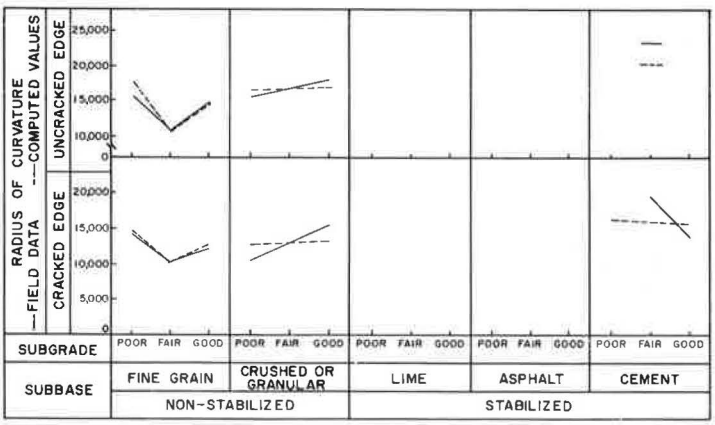

Figure 42. Measured and computed radius of curvatures on high modulus of elasticity concrete.

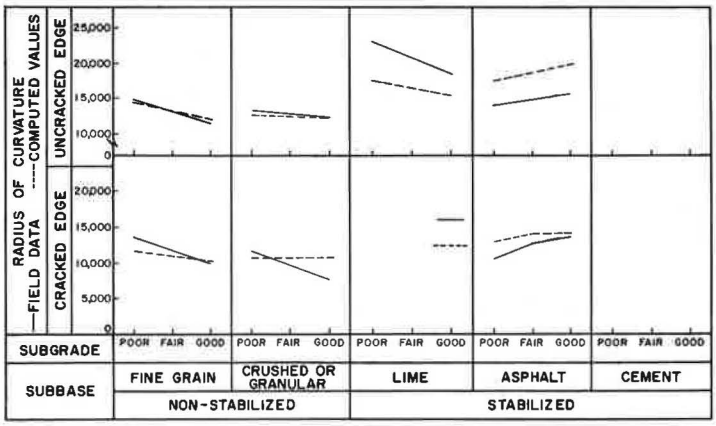

Figure 43. Measured and computed radius of curvatures on low modulus of elasticity concrete.

Final Equation—The radius of curvature equations determined for combined data contained the soil support term. Here again, the definition of soil support can be substituted and the radius of curvature equation will then take the form

$$R_c = \frac{15.3039\ D^{1.75}\ E^{0.3312}\ (U_1 + U_2)^{0.1367}}{L\ T_{sg}^{0.1367}\ \bar{X}^{0.0772}}$$

where all terms are as previously described.

An attempt was made to add the crack width as another variable but the results were such that it would be better not to include the crack width.

Accuracy of Regression Equations

Nineteen sets of deflection and radius of curvature data were analyzed by multiple regression methods. For each analysis a value of r, the correlation coefficient, was obtained. These values of r were checked against a table for their significance for the number of points and degrees of freedom (15). Table 10 gives the results of the r check.

The regression results appear to substantiate the form of the model equations. All checks on the correlation coefficients from the analysis of combined data were above that required to be significant. Previous discussions showed that the standard error of these equations is compatible with the accuracy of the equipment used. Thus the equations are in most cases statistically sound.

TABLE 10

INVESTIGATING THE SIGNIFICANCE OF CORRELATION COEFFICIENTS

Analysis	Crack	Midspan
Deflection:		
Run No. 1	G	F
Run No. 2	G	F
Run No. 3	G	G
Run No. 4	G	G
Combined data	G	G
Radius of Curvature:		
Run No. 1	G	G
Run No. 2	G	F
Run No. 3	G	G
Run No. 4		F
Combined data	G	G

G—The coefficient of correlation is greater than a minimum value required for significance.
F—The coefficient of correlation is less than a minimum value required for significance.

Validation of Design Assumptions

The findings of this study provide validity for the assumptions used in the original design analysis of CRCP. The equal magnitude of deflection at the crack position and midspan position indicates that sufficient granular interlock is provided so that approximately 100 percent load transfer is experienced across a crack. This finding is applicable only where the pavements have 0.5 percent longitudinal steel or more,

although there is a possibility that the lower limit on percent steel may be less than the minimum used in this experiment. Considering these aspects, this finding is applicable over a wide range of support conditions and concrete properties and components.

Furthermore, the use of the Westergaard interior loading conditions for determining the pavement thickness is a satisfactory procedure. The findings of this experiment indicate a 2-in. differential between CRCP and JCP and are in agreement with field performance from a deflection standpoint. This finding also has validity over a wide range of support conditions and concrete properties.

Design Equations

The final equations presented here for both deflection and radius of curvature provide excellent criteria for developing equations to be used in the design of concrete pavements. Although there are numerous factors other than deflection and stress to consider in the design of concrete pavements, this material will present another guideline for a designer to use in selecting the final pavement structure design for a given roadway.

Although percent longitudinal steel and pavement type are not enumerated in these design equations, they may be inserted on the basis of other material and studies developed in connection with this project. These are empirical equations and care should be taken not to extrapolate beyond the limits used in this analysis. The following are some suggested boundary conditions for extrapolation:

D_C = 0.003 in. to 0.030 in.
E = 3×10^6 psi to 6×10^6 psi
D = 6 to 8 in. for CRCP
D = 8 to 10 in. for JCP
$\overline{X}$ = 3 to 12 ft

CONCLUSIONS

This deflection study of CRCP has encompassed a wide variety of conditions and a considerable part of the geographical area of the state. The study was conducted over a 3-year period and over 15,000 separate measurements of various types were used. As a result of this field study and analysis, the following conclusions are warranted:

1. The variables studied herein that were found to affect the deflection of CRCP were concrete modulus of elasticity, modulus of rupture, crack spacing, surface crack width, pavement slab thickness, pavement type, strength characteristics of the subgrade and subbase, and subsurface moisture conditions. An empirical equation was derived using these variables, except modulus of rupture and moisture condition, to predict the deflection of a continuously reinforced concrete pavement under a given wheel load.
2. An equation was also derived from the study that predicts the radius of curvature of a pavement, i.e., related to pavement stress, in terms of the same variables with the exception of crack width.
3. It is recommended that the final equations derived herein be used to develop a nomograph predicting the deflection and radius of curvature for the variables studied. Through the use of this nomograph along with a maximum allowable deflection, pavements may be designed and/or checked in terms of the conditions existing on each project.
4. For the design equation mentioned, the variables of pavement type and percent longitudinal steel may be added to the equation on the basis of the studies herein and previous studies made in connection with this research project.
5. For continuous pavements, longitudinally reinforced with 0.5 percent steel or greater, it was found under a wide variation of support and environmental conditions that the transverse cracks in CRCP are small enough to retain sufficient aggregate interlock to maintain approximately 100 percent load transfer across the crack.
6. The transverse cracks were found to affect the continuity of a CRCP, since measurements indicated that the radius of curvature was smaller, i.e., there was greater stress at the crack than at a midspan point between cracks.
7. From a deflection and stress standpoint, pavements with stabilized subbases are superior in performance to pavements with non-stabilized subbases. All three of the

stabilizing agents considered in this study were found to give excellent performance from a deflection standpoint, but as a result of other studies that will be presented in the future, it is recommended that lime-stabilized subbases be protected with a non-erosive material.

8. From a deflection standpoint, the present practice of using a 2-in. thinner pavement for CRCP in relation to JCP as indicated by current design procedures is correct and conservative. For a given set of conditions, it was found that the deflection for an 8-in. CRCP is equal to or less than for a 10-in. JCP.

9. This study indicated that a reduction in thickness for CRCP had slightly more effect on deflection than an equal reduction in thickness for jointed pavement as found at the AASHO Road Test. Although there is a slight variation, the effect of pavement thickness on deflection as found by (a) this study, (b) the AASHO Road Test, and (c) Westergaard's theoretical analysis are in approximately the same range.

10. The use of a lime-stabilized subgrade, as practiced in Texas, for a working platform or moisture control was found to give an additional benefit of substantially reducing the deflections of a continuous pavement. Under certain conditions, the supporting characteristics of this layer may be considered in design.

11. From a deflection and stress standpoint, the design details presently being used by the Texas Highway Department for CRCP appear to be more than adequate for the conditions found in Texas.

12. This study developed two findings that contradict widely accepted beliefs concerning deflection of concrete pavement: (a) It was found that pavement on moist or saturated foundations deflected less than when the support was dry or partially saturated; These observations were confirmed during two different wet periods and three dry periods. (b) Although the difference is small, deflections and stresses are lower on low modulus CRCP than on high modulus concrete.

ACKNOWLEDGMENTS

The research reported herein was conducted under the supervision of Robert L. Lewis, Research Engineer, and under the general supervision of T. S. Huff, Chief Engineer of Highway Design, Texas Highway Department. The authors wish to extend their thanks to H. D. Swilley, Senior Laboratory Engineer, District 2; B. R. Hunter, Supervising Laboratory Engineer, District 3; Robert L. McKinney, Geologist, District 9; Billy Rudd, Senior Laboratory Engineer, District 10; Franklin J. Shenkir, Senior Laboratory Engineer, District 12; Clarence A. Weise, Supervising Resident Engineer, District 13; Charles W. Baxter, Senior Laboratory Engineer, District 15; Jerry Nemec, Supervising Resident Engineer, District 17; Wilburne C. Gromatsky, Supervising Construction Engineer, District 18; John W. Livingston, Senior Laboratory Engineer, District 19; Warren N. Dudley, Senior Laboratory Engineer, District 20; and Gaston P. Berthelote, Jr., Supervising Resident Engineer, Houston Urban Project, whose cooperation in providing field assistance and basic information made the success of this investigation possible.

The able assistance of various members of the Research Section, Ivan K. Mays, and others who were instrumental in the success of this investigation, is gratefully acknowledged. The field party that gathered the data is also to be commended.

REFERENCES

1. Status Report on Continuously Reinforced Concrete Pavement Built or Under Contract in the U.S. Concrete Reinforcing Steel Institute, July 1966.
2. Shelby, M. D., and McCullough, B. F. Experience in Texas With Continuously Reinforced Concrete Pavement. HRB Bull. 274, p. 1-29, 1960.
3. McCullough, B. F., and Ledbetter, W. B. LTS Design of Continuously Reinforced Concrete Pavements. Jour. Highway Div., Proc. ASCE, Vol. 86, No. HW4, Dec. 1960.
4. AASHO Interim Guide for the Design of Rigid Pavement Structures. AASHO Committee on Design, April 1962.
5. The AASHO Road Test: Report 5, Pavement Research. HRB Spec. Rept. 61E, 1962.

6. McCullough, B. F. Development of Equipment and Techniques for a Statewide Rigid Pavement Deflection Study. Research Rept. No. 46-1, Texas Highway Department, Jan. 1965.
7. McCullough, B. F. Evaluation of Single Axle Load Response on an Experimental Continuously Reinforced Concrete Pavement. Research Rept. No. 46-3, Texas Highway Department, April 1965.
8. McCullough, B. F., and Treybig, H. J. Determining the Relationship of Variables in Deflection of Continuously Reinforced Concrete Pavement. Research Rept. No. 46-4, Texas Highway Department, Aug. 1965.
9. Manual of Testing Procedures, Vol. 1. Texas Highway Department.
10. Design Manual for Controlled Access Highways. Texas Highway Department.
11. Standard Specifications for Road and Bridge Construction. Texas Highway Department, 1962.
12. Hudson, W. R. Value of Single Load Response in Rigid Pavement Design. Paper presented at Texas Section ASCE, May 10, 1963.
13. Taylor, Donald W. Fundamentals of Soil Mechanics (Ninth Printing). John Wiley and Sons, New York, 1956, p. 381-392.
14. McCullough, B. F., and Mays, Ivan K. A Laboratory Study of the Variables That Affect Pavement Deflection. Research Rept. No. 46-6, Texas Highway Department, Aug. 1966.
15. Snedecor, George W. Statistical Methods. Iowa State College Press, Ames, 1946, p. 351.
16. Westergaard, H. M. Stresses in Concrete Pavements Computed by Theoretical Analysis. Public Roads, Vol. 7, No. 2, April 1926.

Editor's Note: The original paper contained six Appendixes pertaining to equipment used, experimental procedure, summaries of data, deflection analysis, and soil support. This material is available from the Highway Research Board at cost of reproduction. When ordering, refer to XS-18, Highway Research Record 239.